

Grid Artifacts Suppression in Computed Radiographic Images

Igor Belykh

Abstract—Anti-scatter grids used in radiographic imaging for the contrast enhancement leave specific artifacts. Those artifacts may be visible or may cause Moiré effect when digital image is resized on a diagnostic monitor. In this paper we propose an automated grid artifacts detection and suppression algorithm which is still an actual problem. Grid artifacts detection is based on statistical approach in spatial domain. Grid artifacts suppression is based on Kaiser bandstop filter transfer function design and application avoiding ringing artifacts. Experimental results are discussed and concluded with description of advantages over existing approaches.

Keywords—Computed radiography, grid artifacts, image filtering.

I. INTRODUCTION

IN modern radiography the reliable diagnostics depends on quality of digital X-ray images. One of the factors that affect image quality is the absence or minimal amount of different type of noise and artifacts. Anti-scatter grids are used in radiology stations [4] for image contrast enhancement but leave visible artifacts that may cause problems while digital image representation for diagnostics.

The use of anti-scatter grids is based on assumptive decomposition of X-ray radiation propagated through the object of interest into a primary and a secondary component. The primary component is formed by the electron beams with small deviations from initial straight line trajectories while secondary component is formed by scattered electrons which are deflected (or even reflected) by object interior. Scattered component degrades image contrast. Anti-scatter grids are designed to enhance image contrast by means of scattered radiation partial reduction and are located between the object and receiving device (Fig. 1), i.e. computed radiography (CR) plate or direct radiography (DR) digital panel [2].

Grid device is a hard plate few millimeters thick (called grid height) with typical dimensions about 14"x17" (35x43 cm) that fit the dimensions of receiving devices. Grids can be stationary or moving during the exposure time, and can be linear or cross and parallel or focused.

Currently stationary linear grids are the most usable [4] and they are the main subject of investigation in this paper. Linear grid structure is similar to jalousie structure with thin stripes made of lead and interspaces filled with aluminum or composite material (Fig. 2).

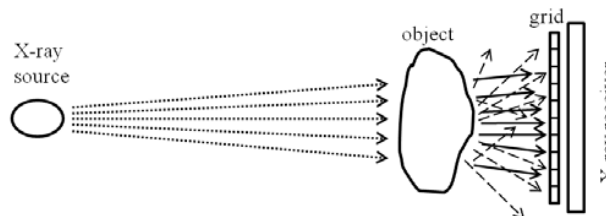


Fig. 1 X-ray image acquisition using anti-scatter grid. Radiation type is denoted by different line style: incident - dotted, primary - solid, scattered - dashed

Primary X-ray beams are mostly transmitted through the grid interspace material while scattered beams along with some primary ones are absorbed by the lead stripes.

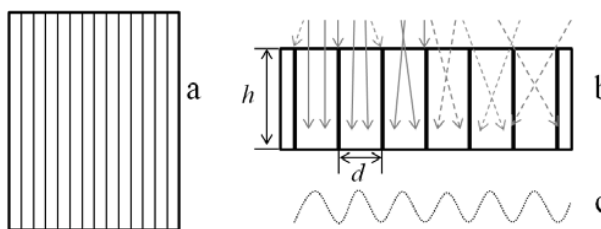


Fig. 2 Linear parallel grid design: a – top view, b – cross-section (solid and dashed arrows denote primary and scattered radiation, respectively). Digital periodic intensity profile (c) registered behind parallel linear grid

Grid stripe thickness is about few hundredth mm and is much smaller than the interspace distance d which is about few tenth mm thick and is much more smaller than grid height h . The h/d ratio is an important grid characteristic and is known as grid ratio with values usually varying in a range of 6 to 16 for different grid design and/or manufacturer. The grid ratio defines a range of spatial angles for the electron trajectories and therefore defines the amount of primary and scattered radiation to be transmitted or absorbed and thus defines the grid effectiveness in image contrast enhancement and finally defines the grid pattern look in registered image. Another important characteristic is the grid stripes' frequency f_g measured in lines per inch (LPI) in a broad range from 85 to 215 LPI. The advantage of the grid use is the higher image contrast but the disadvantages are: the need of higher X-ray dose (up to 3 times) and the visible thin line artifacts that may cause a known Moiré pattern [3] when digital image is resized for display on a diagnostic monitor (Fig. 3).

I. Belykh is with the St. Petersburg State Polytechnical University, St. Petersburg, Russia (phone: +7(812)550-4073; fax: +7(812)703-0202 ext.348; e-mail: igor.belykh@avalon.ru).

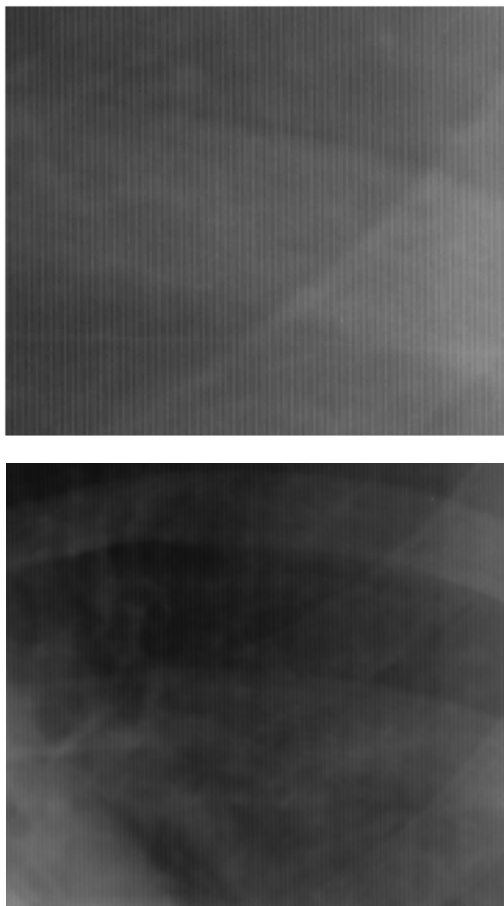


Fig. 3 Line artifacts and Moiré pattern on magnified (upper) and minified (lower) CR image fragments

During the last 10-15 years there were many efforts made to study the grid artifacts and to develop different methods for their detection and suppression. Most of grid detection methods are based on a simple heuristic analysis of the maximum in 1-D Fourier spectrum of image rows/columns providing just a grid frequency [4], [5]. But detection algorithm is supposed to provide accurate and comprehensive information for the suppression algorithm, i.e. not only a grid frequency but some other features that are needed for automated filter design and tuning for the fine elimination of the artifacts preserving the diagnostic quality of the image. The suppression algorithms also were developed by many authors, and most of them suggested the use of two type of filters - lowpass or bandstop – either in spatial [1], [3], [4] or in frequency domains [2] in 1-D or in 2-D [5]. Sasada et al. [5] also suggested a wavelet approach. There are still two main issues needed to be resolved in elimination algorithm. The first one is the use of lowpass filters: they can remove a specified high frequency noise but they blur the image by definition and do not preserve higher frequencies that correspond to objects of small sizes and to diagnostically valuable image background. The second issue is the use of bandstop filters: they suppress narrow-banded noise and

preserve the surrounding frequencies but may produce a visible ringing effect at sharp edges or spikes [1], [2]. Also it's known that Gaussian filters are very inconvenient in accurate tuning to the specific frequency [4]. There are some factors in radiographic acquisition process (we will discuss them later in Section II B) that may cause a 1-D grid detection approaches and further artifacts suppression to be inaccurate or less efficient. Finally, we can summarize that there is still a need for robust and reliable grid artifacts detection and elimination method that will improve but not degrade the diagnostic quality of digital X-ray image.

II. GRID ARTIFACTS DETECTION

A. Grid Artifacts Formation

Grid pattern is formed in radiographic image in two steps. Imagine we acquire the image of the linear parallel grid itself. First, some primary X-ray beams with trajectories sub-parallel (or parallel for focused grid) to grid stripes in source-receiver direction are absorbed when they hit the grid and so leave the line shade right behind the grid stripes (with thickness $t_g \sim 0.05$ mm), forming a minimum of radiation intensity, while in the center of grid interspace there will be a maximum of intensity (Figs. 2 (b),(c)). Due to known [4] geometrical cut-off effect, which is caused by lead stripes absorption depending on grid ratio, the rest of the direct and some scattered beams are registered between the maximal and minimal points forming a periodical structure of radiation intensity behind the grid device with the period T_g . In second step this periodic radiation is either registered by CR plate and then is digitized by a scanner or registered by DR digital detectors.

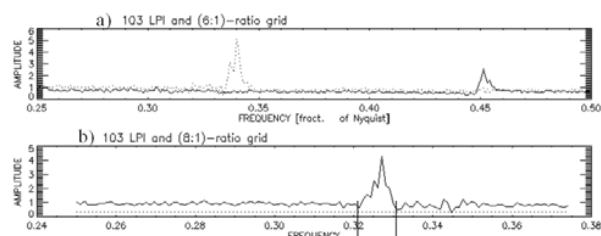


Fig. 4 Fragment of spectra for different grid LPI and ratio (a, b) scanned with different sampling frequency: (a) $f_s = 5.85$ – dotted, and $f_s = 8.7$ – solid; (b) $f_s = 5.85$ - solid, σ -level – dotted, f_1 and f_2 – extracted frequency values of grid maximum width

In both cases the MTFs (Modulation Transfer Functions) of analog and/or digital devices will further smooth the registered radiation field presented by a periodic intensity profile in direction orthogonal to the grid lines (Fig. 2 (c)). That profile is close but not exactly equal to a harmonic function and that is the reason why grid spectral maxima are usually a bit dispersed (Fig. 4 (b)).

The most important point in this digital image acquisition process is that due to the grid fine structure with the frequencies f_g varying in a range of 3.3 to 8.4 lines per mm the sampling frequency f_s according to Nyquist theorem must be

in a range of about 7 to 17 pixels per mm respectively, while in a typical CR station it is about 10 pixels per mm [5]. This means that for some grids there will be spatial frequency aliasing effect that will cause Moiré pattern in registered image. Similar effect may happen for the grids that satisfy the Nyquist requirement at registration stage but cause aliasing when image is minified for display on a monitor.

Since a 2-D grid pattern $g(x,y)$ is a periodic 1-D function $g(x)$ along the x direction, it can be approximated in practice by a finite Fourier sum [2] (phase term is omitted):

$$g(x) = a_0 + \sum_{n=1}^N a_n \cos(2\pi n f_g x) \quad (1)$$

where $a_0 = d/T_g$ (we assume the transmittance coefficient of absorbing material to be equal to zero), a_n represent Fourier series coefficients, where the term with $n=1$ corresponds to grid fundamental frequency and $2f_g, 3f_g, \dots, Nf_g$ are grid harmonic frequencies. If $f_g > f_s/2$ then we have a regular aliasing case and we may see some of grid harmonic maxima in the high frequency area of Fourier spectrum. For instance, if we use a 103 LPI grid and sampling pixel size is 0.115 mm, i.e. $f_g = 4.0$ and $f_s = 8.7$, then Nyquist sampling theorem is satisfied and we expect to see the grid spectral maximum around 0.46. But if we use lower resolution sampling with pixel size of 0.171 mm ($f_s = 5.85$) then Nyquist requirements are not satisfied and we have an aliasing effect, thus we will not expect the grid fundamental frequency in the main period of Fourier spectrum and aliasing frequency of the first order can be estimated [6] as normalized difference $\frac{f_s - f_g}{f_s} = 0.316$.

The positions of maxima discussed above are estimated for the grid device in ideal vertical (or horizontal) position but if it is tilted from the ideal position during the acquisition process then scanning line in CR (or a row/column of digital matrix in DR) and grid stripes will not be perpendicular. That inclination angle β makes a grid frequency lower proportionally to $\cos(\beta)$. Thus the maximum in Fig. 4 (a) (solid line) has the frequency about 0.45 instead of estimated above 0.46 due to inclination of about 10 degrees, analogously aliasing frequency in Fig. 4 (a) (dotted line) instead of calculated above value of 0.316 is around 0.327 due to similar inclination. Another example was shown in [1], where $f_g = 3.3$ and $f_s = 5.8$ and original aliasing frequency should be equal to 0.43 but due to probable grid inclination of about 15 degrees it migrates to the value of 0.45. The inclination effect can make a detection process more complex due to grid spectral maximum variation of shape and position.

Another point for detection algorithm instability is that different body parts (e.g. soft tissue or bones) have different radiation absorption making grid pattern intensity variable and sometimes comparable to noise level and thus making maxima corresponding to grid frequencies hardly noticeable. Those two reasons discussed above require a reliable algorithm invariant to grid inclinations and able to track grid artifacts in images with different body parts and tissues.

B. Grid Artifacts Detection

Since grids require the increase of X-ray dose in some

studies (e.g. in ICU – intensive care units) they are not used, so there is another need to detect whether grid is present or not in acquired image. In this paper we propose the following model for grid artifacts detection that reveals a periodic structure in one dimension and then track it in orthogonal direction. This can be done by calculating an autocorrelation functions (ACF) for each image row and detecting and comparing their dominant periods. If the majority of periods are the same then we make a decision that grid pattern is detected and we can extract its features. Then the process can be repeated for image columns. In order to optimize the process we can compare periods detected in ACF of one row with the ones detected in cross-correlation function (CCF) for a neighbor image rows.

If grid pattern is detected we can extract all features needed for its elimination described below in section 3. We will need the values of grid pattern frequency and magnitude M_g , level of background noise, and the width of spectral maximum.

Grid artifact frequency and magnitude are averaged overall number of spectra of counted image profiles with the detected grid. The level of background noise around each maximum can be estimated as an average standard deviation σ of the right half (high frequency part) of each spectrum. The width of detected maxima can be taken at the level of σ by two frequency values $f1$ (low) and $f2$ (high) averaged overall image profiles (Fig. 4 (b)).

III. GRID ARTIFACTS SUPPRESSION

A. Filter Transfer Function Design

As we mentioned earlier, lowpass filters blur an image and remove high frequencies that provide the presence of image normal background. The removal of that background makes an image look artificial, as in computer graphics, and such images usually are not acceptable by radiologists for clinical diagnostics. Another point is that linear grid patterns are narrow banded and so the bandstop filters are the most appropriate for their suppression by definition. The problem here is a ringing effect especially for narrow banded filters applied to images containing sharp edges and/or spikes. The applied research of the influence of bandstop filter oscillations on image quality is one the subjects of this article. A variety of approaches in digital filter transfer function design and implementation is known, including bandstop filters. Among them is digital filter based on Kaiser transfer function [3], which is the subject of detailed investigation in this paper. The remarkable feature of Kaiser filter is that beside filter length parameter there is another parameter that controls the shape of smoothing window and what is very important the level of Gibbs events [6] that cause periodic oscillations of intensity around narrow band limited by filter stop and pass frequencies. Let us denote full amplitude of Gibbs oscillations as δ and define their desired level as:

$$A = -20 \lg(\delta) \quad (2)$$

Filter length N was empirically defined by Kaiser as a

function of two parameters:

$$N = \frac{(A-7.95)}{28.72 dF} \quad (3)$$

where the width of filter slope can be limited as $dF = \frac{f2-f1}{2}$.

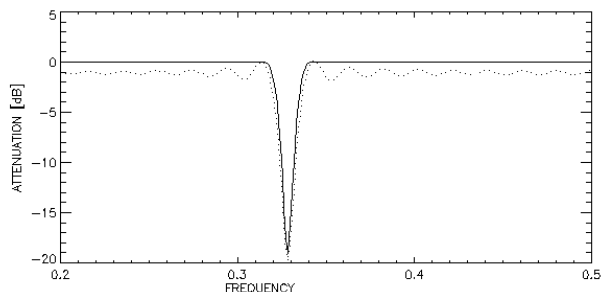


Fig. 5 Fragments of Kaiser transfer function with different A and N values: $A=20$ dB, $N=50$ – dotted line; $A=60$ dB, $N=116$ – solid line

The weights of Kaiser window for $|k| > N$ are set to zero and for $|k| \leq N$ are defined as follows [6]:

$$W_k = \frac{I_0(a \sqrt{1 - (\frac{k}{N})^2})}{I_0(a)} \quad (4)$$

where I_0 – is zero-order Bessel function of the first kind, $a=a(A)$ is a table function of the desired level of Gibbs events empirically defined by Kaiser [6]. Finally, the transfer function is obtained as:

$$H(f) = C_0 + \sum_{k=1}^N C_k(f1, f2) W_k(I_0, a) \cos(2\pi k f) \quad (5)$$

where C_k are coefficients of a known ideal filter rectangular window and depend on stop and pass frequencies $f1$ and $f2$ respectively.

As shown in Fig. 5, we can control the level of oscillations by means of A and N value variations. If we set δ to a constant value then Kaiser window coefficients W_k will be a function of one parameter N , which will affect filter attenuation power and will depend on “grid-to-noise ratio” defined by detector as $20 \lg(\frac{M_g}{\sigma})$. The optimal value for Gibbs events level was estimated experimentally and is equal to $\delta = 0.001$, i.e. $A = 60$ dB (Fig. 5, solid line).

B. Grid Artifacts Filtering

The designed Kaiser bandstop filter was tested on an image fragment similar to represented in [1]. It is reasonable to note that due to the physics of radiographic acquisition all objects are projected onto X-ray receiving device and then digitized, so there are no ideally sharp edges in any registered image object. Even artificial objects located on receiver, such as label “R” with numbers (Fig. 6 (a)), and so the chances of appearance of strong filter ringing are very small. After detection step followed by filtering there are neither visible grid pattern artifacts nor filter ringing effects noticeable neither in filtered magnified image fragment nor in its

spectrum and neither at the edges nor at few visible spikes (Fig. 6 (b)).



Fig. 6 Original (a) and filtered (b) magnified image fragments

Since liner parallel grid pattern is a 1-D structure there is no need to apply a 2-D filter for its elimination. Filtering in a second dimension is reasonable only for the images obtained with cross grids.

IV. RESULTS AND CONCLUSIONS

The implemented grid artifacts detection and suppression method was tested on a representative set of 36 CR images acquired using grids with different frequencies (85, 103, 152 LPI) and ratios (6, 8, 10 and 12) scanned orthogonally with pixel sizes 0.171, 0.115 and 0.097 mm. There was no failure on grid detection and processed images revealed effective grid artifacts suppression preserving acceptable image diagnostic quality as estimated by radiologists.

The proposed grid artifacts elimination method based on Kaiser transfer function demonstrated very reliable and accurate filtering preserving clinically valuable high frequency background structure without ringing and image blur. It is recommended for practical use in CR and DR stations or PACS systems due to the described advantages over existing approaches on theoretical and practical levels.

REFERENCES

- [1] C.Y. Lin, W.J. Lee, S.J. Chen, C.H. Tsai, J.H. Lee, C.H. Chang, Y.T. Ching, "A Study of Grid Artifacts Formation and Elimination in Computed Radiographic Images", *J. Digit. Imaging*, Vol.19, No. 4, December 2006, pp. 351–361.
- [2] D.S. Kim, S. Lee, "Grid artifact reduction for direct digital radiography detectors based on rotated stationary grids with homomorphic filtering", *Med. Phys.*, Vol. 40, No. 6, June 2013, pp.061905-1-061905-14.
- [3] I.N. Belykh, C.W. Cornelius, "Antiscatter stationary grid artifacts automated detection and removal in projection radiography images," in *Proc. SPIE*, 4322, 2001, pp. 1162–1166.
- [4] L.L. Barski, X. Wang, "Characterization, detection and suppression of stationary grids in digital projection radiography imagery", in *Proc. SPIE*, 3658, 1999, pp. 502-519.
- [5] R. Sasada, M. Yamada, S. Hara, H. Takeo, "Stationary grid pattern removal using 2-dimensional technique for Moiré-free radiographic image display", in *Proc. SPIE*, 5029, 2003, pp. 688-698.
- [6] R.W. Hamming, "Digital filters", Prentice-Hall, Englewood Cliffs, 1989.